Journal of Power Sources, 22 (1988) 351 - 357

STRUCTURAL MODELS FOR NICKEL ELECTRODE ACTIVE MASS

B. C. CORNILSEN, P. J. KARJALA and P. L. LOYSELLE

Michigan Technological University, Department of Chemistry and Chemical Engineering, Houghton, MI 49931 (U.S.A.)

Summary

Raman spectroscopic data allow one to distinguish nickel electrode active mass, alpha- and beta-phase materials. Discharged active mass is not isostructural with beta-$Ni(OH)_2$. This is contrary to the generally accepted model for the discharged beta phase of active mass. It is concluded that charged active mass displays a disordered and nonstoichiometric, non-close-packed structure of the $R\bar{3}m$, NiOOH structure type. Raman spectral data and X-ray diffraction data are analyzed and shown to be consistent with this structural model.

Introduction

Raman spectroscopy has proven to be sensitive to subtle structural changes in nickel electrode active mass and related materials. The experimentally observed Raman and IR spectral selection rules provide unique structural information.

Earlier results showed that discharged active mass is not ordered β-$Ni(OH)_2$ [1]. By contrast, the similar selection rules observed for charged and discharged active mass indicated closely-related structures [2]. A structure was proposed for active mass which contains NiO_2 layers in the $R\bar{3}m$ space group, usually referred to as an oxyhydroxide-type structure. The layer–layer stacking is non-close-packed ABBCCA. The crystal structure, together with empirical formulae, define the site occupancy. Nickel vacancies are induced by the nickel deficit nonstoichiometry. Vacancies may be occupied by alkali cations and/or excess protons. The excess protons need not be incorporated as molecular water in this model. Ionization of the vacant cation sites forms Ni(IV) point defects on Ni(III) lattice sites. The nonstoichiometry and dopants control the average nickel oxidation state, and this model explains the maximum values observed empirically.

The presence of point defects increases the disorder of the structure [2]. The nonstoichiometry and point defect content are expected to influence strongly two properties critical to optimum electrochemical performance — proton mobility and electrical conductivity. The enhanced pro-

0378-7753/88/$3.50

perties for the α/γ cycle are consistent with both a larger vacancy content (calculated on the basis of the NiOOH lattice) and the observed spectral shifts [2]. Proposed structures must also be consistent with experimental X-ray powder diffraction patterns.

In this paper we first summarize Raman structural data which allow one to uniquely distinguish active mass, α-, and β-phase materials. This is followed by a structural analysis of charged active mass. Two key structural models of charged active mass will be discussed in terms of the experimental Raman spectra and X-ray powder diffraction patterns. These results show that the structure of charged active mass is non-close-packed with the NiOOH structure.

Experimental

Compounds described in this paper were prepared according to literature methods. Chemical α, first precipitate β-, and recrystallized β-$Ni(OH)_2$ were made as described by Barnard *et al.* [3]. Cathodic α was prepared as described by MacArthur [4]. The discharged α-phase was formed by cycling the cathodic α to -0.2 V in low KOH electrolyte (0.2 M) to prevent β-phase formation [4]. The charged γ-phase was formed by charging the α-phase to +0.51 V in 0.2 M KOH. The preparation method of Bode *et al.* was used to prepare the chemically oxidized, gamma-one material [5]. Potentials were measured and reported with respect to an Hg/HgO/0.2 M KOH reference electrode.

Results

Spectra (a) and (b) in Fig. 1 are typical of cycled active mass. Only two lattice modes are exhibited. No O—H stretches are observed above 3000 cm^{-1}. The charged spectrum is similar to that reported by Jackovitz [6]. This discharged spectrum is reported for the first time. The latter spectrum is different from the spectra of the two β-phases in Fig. 1(c) and (d). Figure 1(e) and (f), of α-phase materials clearly shows that cathodic α and chemical α differ in structure and that neither is the same as discharged active mass. The spectrum of our discharged phase (Fig. 1(b)) differs from Jackovitz's result [1]. The spectrum he reports is similar to that in Fig. 1(d), although only the 3600 cm^{-1} O—H stretch was shown. The spectrum in Fig. 1(d) is that of a first precipitate β-phase. It is not a well-ordered material, as seen by comparison with Fig. 1(c) [3]. The latter is of a recrystallized β-$Ni(OH)_2$. Clearly, Jackovitz's spectrum was of a disordered β, not true β, and not of discharged active mass.

The Raman (Fig. 1(a)) and IR spectra of the charged active mass and the chemically oxidized material are identical, despite the fact that the X-ray pattern of the former material is extensively broadened. This indicates that these two materials are isostructural.

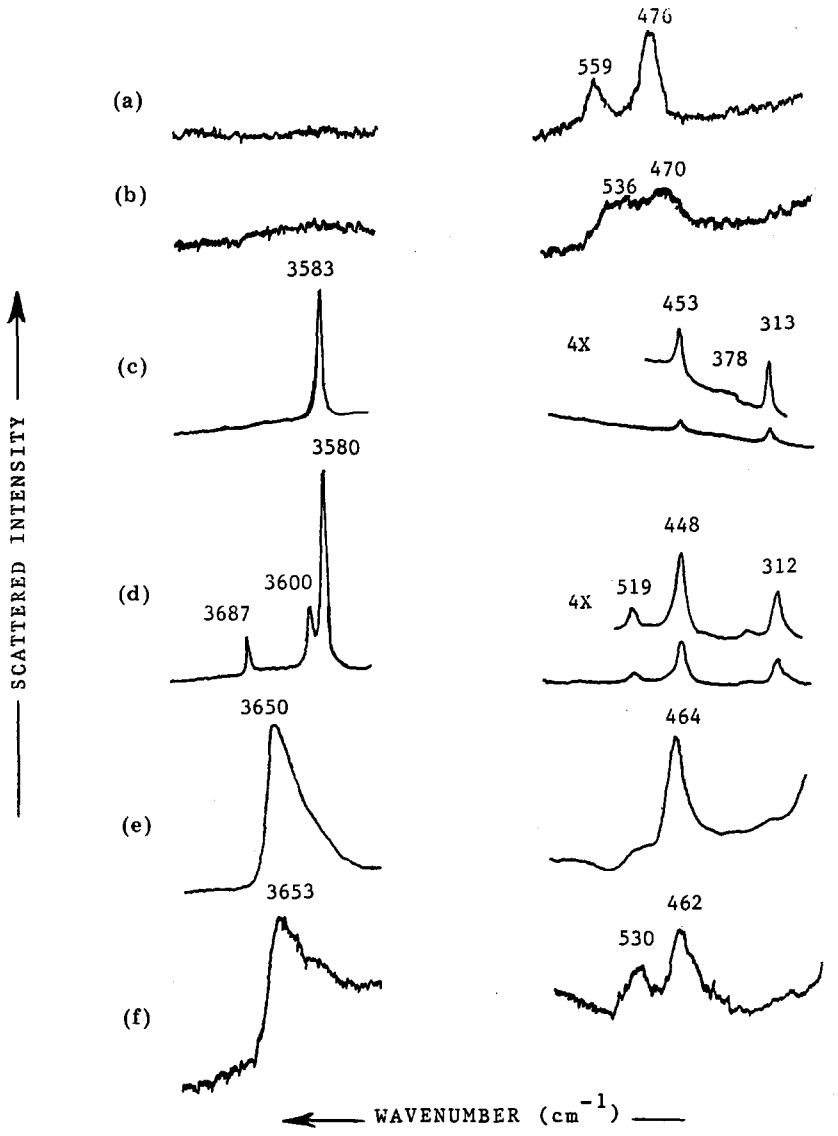

Fig. 1. Raman spectra of nickel electrode active mass and model compounds. (a) Charged γ active mass; (b) discharged α active mass; (c) recrystallized β-$Ni(OH)_2$; (d) first precipitate β-phase; (e) chemical-α; (f) cathodic-α.

A powder pattern of chemically oxidized material (isostructural with charged active mass) shows qualitative agreement with γ-type patterns of Glemser and Einerhand [7] and Bode *et al.* [5] (Table 1). The experimental *d*-spacings agree well, whereas the intensities vary considerably. A re-analysis of these data in terms of the Bode *et al.* *Cm* model (six nickel sites per unit cell) and the $R\bar{3}m$ ($Z = 1$, one nickel site per unit cell) model has been

TABLE 1

Calculated and experimental powder patterns for chemically oxidized material, peak intensities and d spacings

Experimental Bode *et al.**		Experimental this work		Cm model calculation		$R\bar{3}m$ model calculation		
d_{hkl}	I	d_{hkl}	I	d_{hkl}	I	d_{hkl}	I	(hkl)
7.06	100	6.997	100	6.983	100	7.002	100	(003)
				4.252	12			
				4.162	2			
				3.632	4			
3.50	100	3.506	22	3.492	20	3.501	15	(006)
				2.981	1			
2.421	60	2.424	7	2.437	17	2.434	13	(101)
2.366	80	2.379	20	2.389	10	2.387	14	(012)
2.204	40	2.219	1	2.223	9	2.221	9	(104)
				2.126	2			
2.120	90	2.111	12	2.117	14	2.117	10	(105)
				2.112	9			
				2.042	1			
				1.967	1			
1.905	60	1.895	1	1.898	6	1.898	5	(107)
				1.895	5			
1.792	80	1.789	6	1.790	4	1.792	5	(018)
1.754	40			1.746	1			(00$\underline{12}$)
1.601	60	1.595	1	1.594	2	1.595	3	(10$\underline{10}$)
				1.591	2			
1.509	60	1.505	1	1.504	3	1.506	2	(10$\underline{11}$)
				1.418	2			
1.410	80	1.411	5	1.415	2	1.415	2	(00$\underline{15}$)/(110)
				1.397	2			
				1.389	1			
1.385	80	1.383	5	1.387	1	1.387	3	(113)

*Joint Committee for Powder Diffraction Standards, Card No. 23-1407. Interplanar spacings, d_{hkl}, are in Ångströms, and Miller indices are given for the $R\bar{3}m$, hexagonal cell.

carried out. The latter model is consistent with Raman and IR data, the former is not. Calculated values for the $R\bar{3}m$ model show better agreement than the Bode *et al.* unit cell (Table 1). Note that several lines, predicted by the Bode model, are not observed. No discrepancy between observed and calculated lines occurs for the $R\bar{3}m$ model. More importantly, the agreement between observed and experimental intensities is much improved for the $R\bar{3}m$ model.

Theoretical analysis

Raman spectra for β-$Ni(OH)_2$ with the brucite ($P\bar{3}m1 - D^3_{3d}$), $Mg(OH)_2$ structure are expected to display three lattice modes (below 700

cm^{-1}) and one O—H stretch above 3000 cm^{-1}. Spectrum 1(c) of recrystallized β-$Ni(OH)_2$ agrees with these predictions. These selection rules were first predicted for brucite by Mitra [8]. It is well known that β-$Ni(OH)_2$ has the brucite structure [9]. In this structure, the oxygen atoms are hexagonal close packed, ABAB, with nickel atoms in between every other layer.

The second structure of interest is one which exhibits NiO_2 layer stacking that is non-close-packed (*i.e.*, BB, CC or AA). The simplest space group with this packing contains one formula unit ($Z = 1$) of NiO_2H_x with ABBCCA stacking (space group $R\bar{3}m - D_{3d}^5$). A factor group analysis for this model structure predicts only two Raman active lattice modes and no O—H stretching modes for centric H-atoms positioned in the interlamellar space (x can be 1 - 2). The Raman spectra of active mass display selection rules which are consistent with this structure.

Discussion

Figure 1 contains spectra of cycled active mass (charged and discharged), two different β-phase materials, and two different α-phase materials. These six materials each display a different spectrum indicative of a different structure. Each of these materials was prepared according to literature methods to represent either active mass or one of the traditional models for active mass.

Spectra (a) and (b) of Fig. 1, typical of active mass, are clearly different from the β- and α-phases, although to various degrees. Discharged active mass (Fig. 1(b)) and the β-phases ((c) and (d)) are therefore not isostructural. Chemical alpha, cathodic alpha, and discharged active mass (Fig. 1(e), (f) and (b)) also differ in structure. It is apparent that the formation process involves structural transformation from an α- or β-type structure to the active mass structure. Recent *in situ* spectra are consistent with the *ex situ* spectra. More detailed structural analyses of the β- and α-materials will appear in forthcoming publications.

An $R\bar{3}m$, ABBCCA structural model has been proposed for charged active mass [2]. This has been based upon the agreement of the observed Raman selection rules with those predicted for this model. This space group was actually first proposed by Glemser and Einerhand and later interpreted in terms of a larger *Cm* unit cell by Bode *et al.* [7, 5].

The charged active mass structure can be confirmed by X-ray powder pattern analysis. Table 1 shows the experimental and calculated powder patterns for a chemically oxidized material which is isostructural with charged active mass based on IR and Raman spectra. The agreement between calculated and observed d-spacings and peak intensities supports this $R\bar{3}m$ model. The poor agreement between calculated and observed peak intensities and the extra, unobserved peaks calculated for the *Cm*, Bode *et al.*, model, do not compare favorably. This, together with the fact that the vibrational selection rules for the large *Cm* unit cell are not consistent with the observed

spectra, indicates that the $R\bar{3}m$, NiOOH unit cell is the better structural model.

We refer to this as the "charged active mass structure" because the observed Raman and IR selection rules are identical for both charged γ (Fig. 1(a)) and charged β electrochemical materials [2]. The difference between these two materials has been accounted for in terms of this NiOOH lattice and a point defect-containing model [2]. The fundamental difference is in the cation vacancy contents.

Conclusion

The Raman spectral "fingerprints" allow qualitative distinction of several electrode related materials. Structural differences are apparent in the vibrational spectra of nickel electrode active mass and related phases, which were not detected via other techniques such as X-ray diffraction. These differences show that the structures of active mass and those for traditional α and β phases differ. The structural changes which take place during the formation process are mirrored by these differences.

It is concluded that charged active mass is made up of non-close-packed NiO_2 layers (ABBCCA). The Raman spectroscopic and X-ray powder diffraction data are completely consistent with an NiOOH single formula unit cell in the $R\bar{3}m - D_{3d}^5$ space group. This type of stacking encourages the stacking disorder which broadens X-ray patterns. This disorder is combined with point defects which result from extensive cation nonstoichiometry to form excessively disordered materials with unique electrochemical properties.

Acknowledgement

This research has been supported by NASA–Lewis Research Center.

References

1 P. L. Loyselle, D. C. Luehrs and B. C. Cornilsen, Nickel electrode structures, *Extend. Abstr. 168th Electrochem. Soc. Meeting, Las Vegas, NV, October 16, 1985.*

2 P. L. Loyselle, P. J. Karjala and B. C. Cornilsen, in J. R. Selman and H. C. Maru (eds.), *Proc. Symp. on Electrochemical and Thermal Modeling of Battery, Fuel Cell, and Photoenergy Conversion Systems*, Electrochemical Society, Pennington, NJ, 1986, pp. 114 - 121.

3 R. Barnard, C. F. Randell and F. L. Tye, Studies concerning the ageing of alpha and beta $Ni(OH)_2$ in relation to nickel–cadmium cells, in J. Thompson (ed.), *Power Sources 8*, Academic Press, London, 1981, pp. 401 - 423.

4 D. M. MacArthur, The hydrated nickel hydroxide electrode; potential sweep experiments, *J. Electrochem. Soc., 117* (1970) 422 - 426.

5 H. Bartl, H. Bode, G. Sterr and J. Witte, Zur Kenntnis der Nickel Hydroxidelektrode IV. Kristallstrukturuntersuchung des hochoxidierten gamma-one Nickelhydroxids, *Electrochim. Acta, 16* (1973) 615 - 621.
6 J. F. Jackovitz, The vibrational spectra of nickel hydroxide and higher nickel oxide, in R. G. Gunther and S. Gross (eds.), *Proc. Symp. on the Nickel Electrode,* Electrochemical Society, Pennington, NJ, 1982, pp. 48 - 68.
7 O. Glemser and J. Einerhand, Die Struktur hoherer Nickelhydroxyde, *Z. Anorg. Allg. Chem., 261* (1950) 43 - 51.
8 S. S. Mitra, Vibration spectra of solids, in F. Seitz and D. Turnbull (eds.), *Solid State Physics,* 13 (1962) 1 - 80.
9 A. Szytula, A. Murasik and M. Balanda, Neutron diffraction study of $Ni(OH)_2$, *Phys. Status Solidi B, 43* (1971) 125 - 128.